Nodal superconductivity in $Ba(Fe_{1-x}Ru_x)_2As_2$ induced by isovalent Ru substitution

X. Qiu,[1] S. Y. Zhou,[1] H. Zhang,[1] B. Y. Pan,[1] X. C. Hong,[1] Y. F. Dai,[1] Man Jin Eom,[2] Jun Sung Kim,[2] S. Y. Li[1,*]

[1] *Department of Physics, State Key Laboratory of Surface Physics, and Laboratory of Advanced Materials, Fudan University, Shanghai 200433, China*

[2] *Department of Physics, Pohang University of Science and Technology, Pohang 790-784, Korea*

(Dated: July 12, 2011)

We present the ultra-low-temperature heat transport study of an iron-based superconductor $Ba(Fe_{0.64}Ru_{0.36})_2As_2$ (T_c = 20.2 K), in which the superconductivity is induced by isovalent Ru substitution. In zero field we find a large residual linear term κ_0/T, more than 40% of the normal-state value. At low field, the κ_0/T shows an $H^{1/2}$ dependence. These provide strong evidences for nodes in the superconducting gap of $Ba(Fe_{0.64}Ru_{0.36})_2As_2$, which mimics that in another isovalently substituted superconductor $BaFe_2(As_{1-x}P_x)_2$. Our results show that the isovalent Ru substitution can also induce nodal superconductivity in $BaFe_2As_2$, as P does, and they may have the same origin. We further compare them with other two nodal superconductors LaFePO and LiFeP.

PACS numbers: 74.70.Xa, 74.25.fc, 74.20.Rp

Since the discovery of high-T_c superconductivity in iron-based compounds [1, 2], the electronic pairing mechanism has been a central issue [3]. One key to understand it is to clarify the symmetry and structure of the superconducting gap [4]. However, even for the most studied (Ba,Sr,Ca,Eu)Fe_2As_2 (122) system, the situation is still fairly complex [4].

Near optimal doping, for both hole- and electron-doped 122 compounds, the angle-resolved photon emission spectroscopy (ARPES) experiments clearly demonstrated multiple nodeless superconducting gaps [5, 6], which was further supported by bulk measurements such as thermal conductivity [7–9]. On the overdoped side, nodal superconductivity was found in the extremely hole-doped KFe_2As_2 [10, 11], while strongly anisotropic gap [9], or isotropic gaps with significantly different magnitude [12, 13] were suggested in the heavily electron-doped $Ba(Fe_{1-x}Co_x)_2As_2$. On the underdoped side, recent heat transport measurements claimed possible nodes in the superconducting gap of hole-doped $Ba_{1-x}K_xFe_2As_2$ with $x < 0.16$ [14], in contrast to the nodeless gaps found in electron-doped $Ba(Fe_{1-x}Co_x)_2As_2$ [9].

Intriguingly, nodal superconductivity was also found in $BaFe_2(As_{1-x}P_x)_2$ (T_c = 30 K) [15, 16], in which the superconductivity is induced by the isovalent P substitution for As. The laser-ARPES experiments on $BaFe_2(As_{0.65}P_{0.35})_2$ showed isotropic gaps in the three hole pockets around the Brillouin zone (BZ) center, therefore the gap nodes must locate on the electron pockets around the BZ corners [17]. Moreover, previously LaFePO ($T_c \sim$ 6 K) displays clear nodal behavior [18–20], and recently there is penetration depth evidence for nodes in the superconducting gap of LiFeP ($T_c \sim$ 4.5 K) [21]. The nodal superconductivity in these P-substituted compounds are very striking, which raises the puzzling question why the P substitution is so special in iron-based superconductors. The theoretical explanations of this puzzle are far from consensus [22–25].

In the Fe_2As_2 slabs of iron arsenides shown in Fig. 1, instead of substituting As with P, there is an alternative way for isovalent substitution, to substitute Fe with Ru. Indeed, superconductivity with T_c up to 20 K was found in $Ba(Fe_{1-x}Ru_x)_2As_2$ [26] and $Sr(Fe_{1-x}Ru_x)_2As_2$ [27]. The phase diagram of $Ba(Fe_{1-x}Ru_x)_2As_2$ is very similar to that of $BaFe_2(As_{1-x}P_x)_2$ [28, 29]. The ARPES measurements on $Ba(Fe_{0.65}Ru_{0.35})_2As_2$ showed that Ru induces neither hole nor electron doping, but the hole and electron pockets are about twice larger than in $BaFe_2As_2$ [30]. To investigate the superconducting gap structure in these Ru-substituted superconductors may help to solve above puzzle of P substitution.

In this Letter, we report the demonstration of nodal superconductivity in optimally substituted $Ba(Fe_{0.64}Ru_{0.36})_2As_2$ by thermal conductivity measurements down to 50 mK. Our finding shows that the nodal superconducting states in P-substituted iron arsenides are not that special, and suggests a common origin of the nodal superconductivity induced by isovalent substitutions, at least in $Ba(Fe_{1-x}Ru_x)_2As_2$ and $BaFe_2(As_{1-x}P_x)_2$.

Single crystals of optimally substituted $Ba(Fe_{0.64}Ru_{0.36})_2As_2$ were grown using a self-flux method [31]. Plate-shaped crystals with shiny surfaces were extracted mechanically. The Ru substituting level was determined by energy dispersive X-ray spectroscopy. The dc magnetic susceptibility was measured at H = 10 Oe, with zero-field cooled, using a SQUID (MPMS, Quantum Design). The sample was cleaved to a rectangular shape of dimensions 1.50 × 0.68 mm^2 in the ab-plane, with 70 μm thickness along the c-axis. Contacts were made directly on the sample surfaces with silver paint, which were used for both resistivity and thermal conductivity measurements. The contacts are metallic with typical resistance 200 mΩ at 1.5 K. In-plane thermal conductivity was measured in a dilution refrigerator, using a standard four-wire

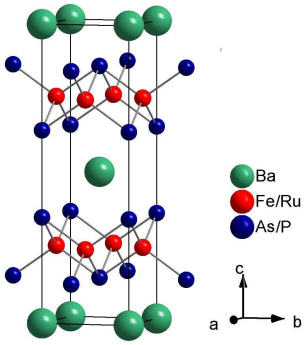

FIG. 1: (Color online). Crystal structure of $BaFe_2As_2$. There are two ways for isovalent substitution in the Fe_2As_2 slabs, substituting As with P, or Fe with Ru. Both substitutions can induce superconductivity, and result in similar phase diagrams.

steady-state method with two RuO_2 chip thermometers, calibrated *in situ* against a reference RuO_2 thermometer. Magnetic fields were applied along the c-axis. To ensure a homogeneous field distribution in the sample, all fields were applied at temperature above T_c.

Fig. 2a shows the in-plane resistivity $\rho(T)$ of our $Ba(Fe_{0.64}Ru_{0.36})_2As_2$ single crystal. The magnitude and shape of $\rho(T)$ are consistent with previous report [28]. The normalized magnetization was plotted in the inset, which displays a nice superconducting transition at about 20 K. According to the phase diagram of $Ba(Fe_{1-x}Ru_x)_2As_2$ [28, 29], no static magnetic order exists in our optimally substituted sample. The resistivity data between 30 and 90 K are fitted to $\rho(T) = \rho_0 + AT^n$, which gives a residual resistivity $\rho_0 = 43.7 \pm 0.1$ $\mu\Omega$cm and $n = 1.31 \pm 0.1$. Such a non-Fermi-liquid temperature dependence of $\rho(T)$ is similar to that observed in $BaFe_2(As_{1-x}P_x)_2$ near optimal substitution, which may reflet the presence of antiferromagnetic spin fluctuations near a quantum critical point [32].

The low-temperature part of $\rho(T)$ is plotted in Fig. 2b. The zero-resistance point of the resistive transition is at $T_c = 20.2$ K, which is in good agreement with the diamagnetic superconducting transition shown in the inset of Fig. 2a. To estimate the upper critical field H_{c2}, the resistivity in $H = 3$, 6, 9, and 14.5 T with $H||c$ were also measured, as seen in Fig. 2b. Fig. 2c shows the temperature dependence of H_{c2}, defined by $\rho = 0$ and $\rho = 0.1\rho_N$, respectively. For comparison, the $H_{c2}(T)$ of the electron-doped $Ba(Fe_{0.9}Co_{0.1})_2As_2$ single crystal with $T_c \approx 22$ K is reproduced from ref. [33]. One can see that although the T_c of our $Ba(Fe_{0.64}Ru_{0.36})_2As_2$ is only slightly lower than $Ba(Fe_{0.9}Co_{0.1})_2As_2$, its $H_{c2}(T)$ is significantly lower. For $Ba(Fe_{0.9}Co_{0.1})_2As_2$, extrapolation of the $H_{c2}(T)$ data suggests $H_{c2}(0)$ between 40 and 50 T, much larger than that obtained from Werthamer-Helfand-Hohenberg formula $H_{c2}^{WHH}(0) = -0.69T_c dH_{c2}/dT|_{T=T_c}$ [33]. For our

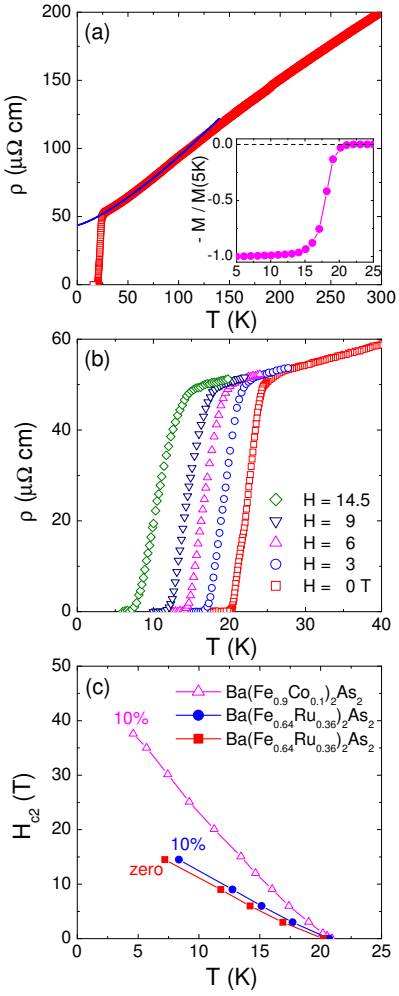

FIG. 2: (Color online). (a) In-plane resistivity of $Ba(Fe_{0.64}Ru_{0.36})_2As_2$ single crystal. The solid line is a fit of the data between 30 and 90 K to $\rho(T) = \rho_0 + AT^n$. Inset: normalized magnetization. (b) Low-temperature resistivity in $H = 0$, 3, 6, 9, and 14.5 T with $H||c$. (c) Temperature dependence of the upper critical field H_{c2}. The squares and circles represent H_{c2} of $Ba(Fe_{0.64}Ru_{0.36})_2As_2$ defined by $\rho = 0$ and $\rho = 0.1\rho_N$, respectively. The triangles represent H_{c2} of $Ba(Fe_{0.9}Co_{0.1})_2As_2$ with $T_c \approx 22$ K [33].

$Ba(Fe_{0.64}Ru_{0.36})_2As_2$, $H_{c2}^{WHH}(0) \approx 15.3$ T is obtained, which is also apparently lower than the actual $H_{c2}(0)$. We can only roughly estimate the bulk $H_{c2}(0) \approx 23$ T, defined by $\rho = 0$, by linearly extrapolating the data between 6 and 14.5 T in Fig. 2c. Note that a slightly different $H_{c2}(0)$ does not affect our discussion below.

Fig. 3 shows the temperature dependence of the in-plane thermal conductivity for $Ba(Fe_{0.64}Ru_{0.36})_2As_2$ in $H = 0$, 1, 2, 4, 6, 9, and 12 T magnetic fields, plotted as κ/T vs T. All the curves are roughly linear, as previously observed in $BaFe_{1.9}Ni_{0.1}As_2$ [8], KFe_2As_2 [10], and overdoped $Ba(Fe_{1-x}Co_x)_2As_2$ single crystals [9, 12]. Therefore we fit all the curves to $\kappa/T = a + bT^{\alpha-1}$ with α fixed to 2. The two terms aT and bT^{α} represent contri-

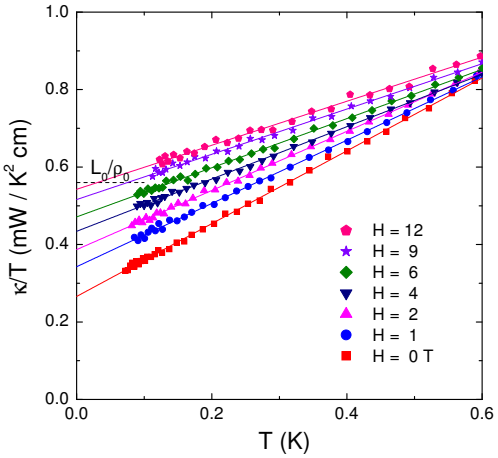

FIG. 3: (Color online). Low-temperature in-plane thermal conductivity of $Ba(Fe_{0.64}Ru_{0.36})_2As_2$ in magnetic fields applied along the c-axis (H = 0, 1, 2, 4, 6, 9 and 12 T). The solid lines are $\kappa/T = a + bT$ fit to all the curves, respectively. The dash line is the normal-state Wiedemann-Franz law expectation L_0/ρ_0, with L_0 the Lorenz number 2.45 $\times$ 10^{-8} $W\Omega K^{-2}$ and ρ_0 = 43.7 $\mu\Omega$cm.

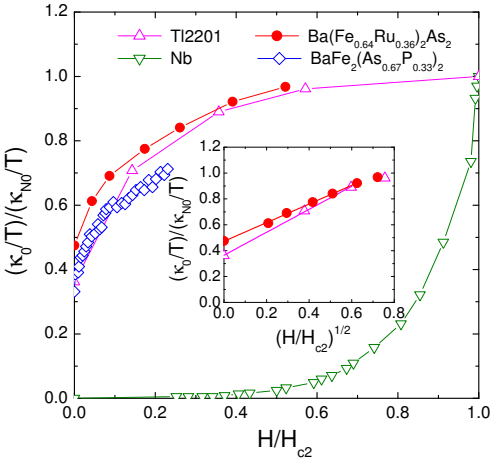

FIG. 4: (Color online). Normalized residual linear term κ_0/T of $Ba(Fe_{0.64}Ru_{0.36})_2As_2$ as a function of H/H_{c2}. Similar data of the clean s-wave superconductor Nb [35], an overdoped d-wave cuprate superconductor Tl-2201 [36], and $BaFe_2(As_{0.67}P_{0.33})_2$ [16] are also shown for comparison. The behavior of $\kappa_0(H)/T$ in $Ba(Fe_{0.64}Ru_{0.36})_2As_2$ clearly mimics that in Tl-2201 and $BaFe_2(As_{0.67}P_{0.33})_2$. Inset: the same data of $Ba(Fe_{0.64}Ru_{0.36})_2As_2$ and Tl-2201 plotted against $(H/H_{c2})^{1/2}$. The lines represent the $H^{1/2}$ dependence.

butions from electrons and phonons, respectively. Here we only focus on the electronic term.

In zero field, the fitting gives a residual linear term κ_0/T = 0.266 $\pm$ 0.002 mW K^{-2} cm^{-1}. This value is more than 40% of the normal-state Wiedemann-Franz law expectation $\kappa_{N0}/T = L_0/\rho_0$ = 0.56 mW K^{-2} cm^{-1}, with L_0 the Lorenz number 2.45 $\times$ 10^{-8} $W\Omega K^{-2}$ and ρ_0 = 43.7 $\mu\Omega$cm. For another isovalently substituted $BaFe_2(As_{0.67}P_{0.33})_2$ single crystal, similar value of $\kappa_0/T \approx 0.25$ mW K^{-2} cm^{-1} was obtained, which is about 30% of its normal-state κ_{N0}/T [16]. The significant κ_0/T of $Ba(Fe_{0.64}Ru_{0.36})_2As_2$ in zero field is a strong evidence for nodes in the superconducting gap [34].

The field dependence of κ_0/T may provide further support for the nodes [34]. In Fig. 4, the normalized $(\kappa_0/T)/(\kappa_{N0}/T)$ of $Ba(Fe_{0.64}Ru_{0.36})_2As_2$ is plotted as a function of H/H_{c2}, with the normal-state κ_{N0}/T = 0.56 mW K^{-2} cm^{-1} and bulk H_{c2} = 23 T. Similar data of the clean s-wave superconductor Nb [35], an overdoped d-wave cuprate superconductor Tl-2201 [36], and $BaFe_2(As_{0.67}P_{0.33})_2$ [16] are also plotted for comparison. For a nodal superconductor in magnetic field, delocalized states exist out the vortex cores and dominate the heat transport in the vortex state, in contrast to the s-wave superconductor. At low field, the Doppler shift due to superfluid flow around the vortices will yield an $H^{1/2}$ growth in quasiparticle density of states (the Volovik effect [37]), thus the $H^{1/2}$ field dependence of κ_0/T. From Fig. 4, the behavior of $\kappa_0(H)/T$ in $Ba(Fe_{0.64}Ru_{0.36})_2As_2$ clearly mimics that in Tl-2201 and $BaFe_2(As_{0.67}P_{0.33})_2$. In the inset of Fig. 4, the $\kappa_0(H)/T$ of $Ba(Fe_{0.64}Ru_{0.36})_2As_2$ obeys the $H^{1/2}$ dependence at low field, which supports the existence of nodes in the superconducting gap.

To our knowledge, previously there are five iron-based superconductors displaying nodal superconductivity, KFe_2As_2 [10, 11], underdoped $Ba_{1-x}K_xFe_2As_2$ ($x <$ 0.16) [14], $BaFe_2(As_{1-x}P_x)_2$ [15, 16], LaFePO [18–20], and LiFeP [21]. Here we only consider the "in-plane nodes", not counting the "c-axis nodes" in underdoped and overdoped $Ba(Fe_{1-x}Co_x)_2As_2$ as suggested by c-axis heat transport experiments [38]. For the extremely hole-doped KFe_2As_2, the nodal superconductivity may result from the intraband pairing via antiferromagnetic fluctuations, due to the lack of electron pockets [10]. For underdoped $Ba_{1-x}K_xFe_2As_2$, it is still not clear how the superconducting gap transforms from nodeless to nodal at $x \approx 0.16$ [14]. The rest three compounds, $BaFe_2(As_{1-x}P_x)_2$, LaFePO, and LiFeP, have stimulated various interpretations of the effect of isovalent P substitution on the superconducting gap structure [22–25].

Our new finding of nodal superconductivity in $Ba(Fe_{0.64}Ru_{0.36})_2As_2$ reveals the similarity between the isovalently Ru- and P-substituted iron arsenides, therefore the P substitution is not that special for inducing nodal superconductivity. In this sense, the mystery of P substitution in iron-based superconductors has been partially unwrapped. What next one needs to do is to find out whether there is a common origin for the nodal superconductivity in these isovalently substituted compounds.

Due to the smaller size of P ion than As ion, one common structural feature of the P-substituted compounds is the decrease of pnictogen height and increase of As-Fe-

As angle [32, 40, 41]. The substitution of larger Ru ion for Fe ion in $Ba(Fe_{1-x}Ru_x)_2As_2$ results in the increase of a lattice parameter and decrease of c lattice parameter, thus the decrease of pnictogen height and increase of As-Fe-As angle too [28]. Therefore, both the P and Ru substitutions cause the same trend of structure change in iron arsenides.

LaFePO and LiFeP belong to the "1111" and "111" systems, respectively, and the P ions have fully substituted As ions in LaFeAsO and LiFeAs. This is different from the partial P and Ru substitution in superconducting $BaFe_2(As_{1-x}P_x)_2$ and $Ba(Fe_{1-x}Ru_x)_2As_2$. In fact, both the fully substituted $BaFe_2P_2$ and $BaRu_2As_2$ are nonsuperconducting [42, 43]. Another difference is the much lower T_c of LaFePO and LiFeP, 6 and 4.5 K, respectively. For LaFePO, Kuroki *et al.* have attributed the low-T_c nodal pairing to the lack of Fermi surface γ around (π, π) in the unfolded Brillouin zone, due to the low pnictogen height [22]. Hashimoto *et al.* also related the nodal superconductivity in LiFeP to the pnictogen height [21].

For $Ba(Fe_{1-x}Ru_x)_2As_2$ and $BaFe_2(As_{1-x}P_x)_2$, the substitutions start from the same parent compound $BaFe_2As_2$, and result in similar phase diagrams [28, 29]. The highest T_c at optimal substitution, 20 and 30 K, are also close. Furthermore, the Fermi surface structures are roughly similar, with hole pockets around BZ center and electron pockets around BZ corners [17, 30]. All these similarities suggest that the origin of the nodal superconductivity in $Ba(Fe_{1-x}Ru_x)_2As_2$ and $BaFe_2(As_{1-x}P_x)_2$ may be the same. Suzuki *et al.* have proposed three-dimensional nodal structure in the largely warped hole Fermi surface and no nodes on the electron Fermi surface [25]. However, these seem inconsistent with the ARPES results, which have constrained the nodes on the electron pockets [17]. More careful considerations of the structural parameters, band structure, and local interactions are needed to clarify whether there is a common origin for the nodal superconductivity in all these isovalently substituted iron arsenides.

In summary, we have measured the thermal conductivity of $Ba(Fe_{0.64}Ru_{0.36})_2As_2$ single crystal down to 50 mK. A large κ_0/T at zero field and an $H^{1/2}$ field dependence of $\kappa_0(H)/T$ at low field give strong evidences for nodal superconductivity in $Ba(Fe_{0.64}Ru_{0.36})_2As_2$. Comparing with previous P-substituted iron arsenides, our new finding suggest that the nodal superconductivity induced by isovalent substitutions may have the same origin, at least in $Ba(Fe_{1-x}Ru_x)_2As_2$ and $BaFe_2(As_{1-x}P_x)_2$. Finding out this origin will be important for getting a complete electronic pairing mechanism of the iron-based high-T_c superconductors.

This work is supported by the Natural Science Foundation of China, the Ministry of Science and Technology of China (National Basic Research Program No: 2009CB929203), Program for New Century Excellent Talents in University, Program for Professor of Special Appointment (Eastern Scholar) at Shanghai Institutions of Higher Learning, and STCSM of China (No: 08dj1400200 and 08PJ1402100).

* E-mail: shiyan_li@fudan.edu.cn

[1] Y. Kamihara *et al.*, J. Am. Chem. Soc. **130**, 3296 (2008).
[2] J. Paglione and R. L. Greene, Nature Physics **6**, 645 (2010).
[3] Fa Wang and Dung-hai Lee, Science **332**, 200 (2011).
[4] P. J. Hirschfeld, M. M. Korshunov, and I. I. Mazin, arXiv:1106.3712, and references therein.
[5] H. Ding *et al.*, EPL **83**, 47001 (2008).
[6] K. Terashima *et al.*, Proc. Natl. Acad. Sci. **106**, 7330 (2009).
[7] X. G. Luo *et al.*, Phys. Rev. B **80**, 140503(R) (2009).
[8] L. Ding *et al.*, New J. Phys. **11**, 093018 (2009).
[9] M. A. Tanatar *et al.*, Phys. Rev. Lett. **104**, 067002 (2010).
[10] J. K. Dong *et al.*, Phys. Rev. Lett. **104**, 087005 (2010).
[11] K. Hashimoto *et al.*, Phys. Rev. B **82**, 014526 (2010).
[12] J. K. Dong *et al.*, Phys. Rev. B **81**, 094520 (2010).
[13] Yunkyu Bang, Phys. Rev. Lett. **104**, 217001 (2010).
[14] J.-Ph. Reid *et al.*, arXiv:1105.2232.
[15] Y. Nakai *et al.*, Phys. Rev. B **81**, 020503(R) (2010).
[16] K. Hashimoto *et al.*, Phys. Rev. B **81**, 220501(R) (2010).
[17] T. Shimojima *et al.*, Science **332**, 564 (2011).
[18] J. D. Fletcher *et al.*, Phys. Rev. Lett. **102**, 147001 (2009).
[19] C. W. Hicks *et al.*, Phys. Rev. Lett. **103**, 127003 (2009).
[20] M. Yamashida *et al.*, Phys. Rev. B **80**, 220509 (2009).
[21] K. Hashimoto *et al.*, to be published.
[22] K. Kuroki *et al.*, Phys. Rev. B **79**, 224511 (2009).
[23] F. Wang, H. Zhai, and D.-H. Lee, Phys. Rev. B **81**, 184512 (2010).
[24] R. Thomale *et al.*, Phys. Rev. Lett. **106**, 187003 (2011).
[25] K. Suzuki, H. Usui, and K. Kuroki, J. Phys. Soc. Jpn. **80**, 013710 (2011).
[26] S. Sharma *et al.*, Phys. Rev. B **81**, 174512 (2010).
[27] W. Schnelle *et al.*, Phys. Rev. B **79**, 214516 (2009).
[28] F. Rullier-Albenque *et al.*, Phys. Rev. B **81**, 224503 (2010).
[29] A. Thaler *et al.*, Phys. Rev. B **82**, 014534 (2010).
[30] V. Brouet *et al.*, Phys. Rev. Lett. **105**, 087001 (2010).
[31] Man Jin Eom and Jun Sung Kim, to be published.
[32] S. Kasahara *et al.*, Phys. Rev. B **81**, 184519 (2010).
[33] A. Yamamoto *et al.*, Appl. Phys. Lett. **94**, 062511 (2009).
[34] H. Shakeripour *et al.*, New J. Phys. **11**, 055065 (2009).
[35] J. Lowell and J. Sousa, J. Low. Temp. Phys. **3**, 65 (1970).
[36] C. Proust *et al.*, Phys. Rev. Lett. **89**, 147003 (2002).
[37] G. E. Volovik, JETP Lett. **58**, 469 (1993).
[38] J.-Ph. Reid *et al.*, Phys. Rev. B **82**, 064501 (2010).
[39] W. K. Yeoh *et al.*, Phys. Rev. Lett. **106**, 247002 (2011).
[40] M. Tegel *et al.*, arXiv:0805.1208, Z. Naturforsch. B - Chem. Sci. **63**, 1057 (2008).
[41] S. Jiang *et al.*, J. Phys. Condens. Matter **21**, 382203 (2009).
[42] H. Shishido *et al.*, Phys. Rev. Lett. **104**, 057008 (2010).
[43] R. Nath *et al.*, Phys. Rev. B **79**, 174513 (2009).